

BEHAVIOUR AND OPTIMISATION OF MULTI-DIRECTIONAL LAMINATE SPECIMENS UNDER DELAMINATION BY BENDING

VEDENJE IN OPTIMIZACIJA VEČSMERNIH VZORCEV LAMINATOV PRI UPOGIBU Z DELAMINACIJO

Nourdine Ouali¹, Ali Ahmed-Benyahia¹, Abdelouahed Laksimi², Taoufik Boukharouba¹

¹ Laboratoire de Mécanique Avancée (LMA), F GM&GP de l'USTHB, BP. 32 El-Alia 1111 Alger, Algérie

² Laboratoire des Polymères et Composites, Université de Technologie de Compiègne, France
abenyahiaa@yahoo.fr

Prejem rokopisa – received: 2006-05-17; sprejem za objavo – accepted for publication: 2006-07-24

This work forms part of a study of the behaviour and characterisation of a ($\pm\theta$) multi-directional glass/epoxy composite loaded in modes I and II by bending. For the mode I loading the tests were performed on double cantilever beam (DCB) specimens. These tests resulted in two types of delamination: delamination in the median plan for the low angles ($\theta \leq 33.5^\circ$) and a delamination in staircases for the high angles ($33.5^\circ \leq \theta \leq 67.5^\circ$). The delamination in staircases creates an unsymmetrical specimen that generates a shear effort in the crack tip and the loading can no longer be considered as pure mode I, but rather a mixed mode (I + II) and sometimes mode (I + II + III). The starting-energy release rate and the propagation energy are often difficult to characterise for these materials, because the start of the delamination is preceded by a transverse cracking of the most tensed plies if the specimen test thickness is relatively weak, and in the propagation phase, the delamination is accompanied by a large rate of transversal cracks. For the low angles, exposed fibres and imprints of fibres is the aspect that dominates the fracture surfaces. Occasional broken fibres and cusps at the intersections of the plan of the rupture with the wefts were also observed. For the large angles, the number of broken fibres is more important than in the case of low angles. A thickness optimisation of the DCB specimen was made in order to avoid the appearance of transverse cracking before the start of the delamination.

Keywords: delamination, multi-directional laminate, energy release rate, crack propagation, fibre orientation, optimisation.

V tem delu je predstavljen del raziskave vedenja in karakterizacije ($\pm\theta$) večsmernih kompozitov steklo-epoksi, obremenjenih na upogib na način I ali II. Pri načinu I so bili preizkusi obremenitve izvršeni na dvojnih konzolnih nosilcih (DCB). Pri teh preizkusih sta se pojavili dve vrsti delaminacije: delaminacija v osrednji ravnini pri majhnih kotih ($\theta \leq 35^\circ$) in stopničasta delaminacija pri velikih kotih ($33,5^\circ \leq \theta \leq 67,5^\circ$). Pri tej delaminaciji je nastal asimetrični preizkušanelec, ki je ustvaril strig v konici razpoke, zato obremenitev ni bila več čiste vrste I, ampak mešane vrste (I + II), včasih celo (I + II + III). Za te materiale je pogosto težko opredeliti hitrost sprostitve začetne energije in energijo propagacije, ker pred delaminacijo nastanejo prečne razpoke na najbolj obremenjenih plasteh, in če je preizkušanelec relativno tanek, pri prapagaciji delaminacijo spremlja velika hitrost nastajanja prečnih razpok. Za majhne kote so značilnost preloma gola vlakna in odtisi teh vlaken. Občasno smo opazili tudi prelomljena vlakna in konice na presečišču ravnine preloma in prečnih vlaken. Pri velikem kotu je število zlomljenih vlaken večje kot pri majhnih kotih. Optimizacije debeline DCB-preizkušanca je bila pripravljena z namenom, da bi preprečili prečno pokanje pred delaminacijo.

Ključne besede: delaminacija, večsmern laminat, energija, hitrost sprostitve, propagacija razpoke, orientacija vlaken, optimizacija

1 INTRODUCTION

The various configurations and the various methods of calculation of the fracture toughness G for composite laminates were often developed for unidirectional laminates and all the research carried out in the field of multidirectional laminates uses the same configurations and the same methods of calculation³.

The published literature⁷⁻⁸ shows that practically all the works that approach the effect of the plies orientation on the energy release rate in propagation are limited to the effect of the interface of the initial crack. Thus some authors do not judge it necessary to present the sequences of stratification used in their studies. They present only the interfaces containing the initial crack. This is why we carried out the present work, to elucidate the effect of the stratification sequence on the fracture

mode and the evolution of the propagating energy in the case of multi-directional laminates $\pm\theta$ loaded in mode I by bending using the DCB specimen.

The method of experimental compliance is used to determine the critical energy of the start of delamination, G_{IC} . For the energy of propagation G_{IP} , three methods of calculation are used: the technique of the R -curve, experimental compliance by loading-unloading, and the area method. A comparison of the results of these three methods will be carried out.

However, some researches¹⁰⁻¹² using the DCB specimen showed that the clamping of the arms at the crack tip was not as perfect as it is supposed to be and made a correction to the formulation of the analytical compliance by adding a term that accounts for the angle of the deflection of the arms at the crack tip. Reference¹³ highlighted non-linearities of the behaviour related to

large displacements and the excessive angle of deflection. These problems of partial clamping of the arms and non-linearity affect the behaviour of the multi-directional composites by generating additional dissipative phenomena such as the transverse cracking of the plies tensed in the case of large angles of the fibres' orientation^{1,3}. These problems also generate some difficulties in the analysis of the experimental characterization results.

We think that these problems depend on the specimen thickness. Thus, we propose in this study to identify these problems and to find the relation which binds them to the thickness of the DCB specimen. Finally, we propose an optimisation of this thickness that would prevent these dissipative phenomena from occurring before the start of delamination, without which any characterization would be erroneous.

The mechanical tests were performed in the polymers and composites laboratory of Compiegne University, France.

2 MATERIAL AND EXPERIMENTAL CONDITIONS

The material used in this study was a glass E/resin composite (Vicotex M10) moulded in an autoclave (1H with 120°, under pressure 0.85 bar, over pressure 3 bar). The elementary plies were almost uni-directional (5% fibre in the perpendicular direction). The mechanical characteristics of the unidirectional laminate are summarised in **Table 1**.

Table 1: Mechanical characteristics of the unidirectional laminate
Tabela 1: Mehanske značilnosti enosmernege laminata

E_{xx} /GPa	E_{yy} /GPa	G_{xy} /GPa	ν_{xy}
44.11 ± 3.22	17.98 ± 1.67	6.16 ± 0.24	0.267 ± 0.005

The tested laminates were draped from pre-impregnated plies in a multidirectional manner. The stacking sequence was selected in the form $[(+\theta/-\theta)]$ with four different configurations: $\theta = 15^\circ, 30^\circ, 45^\circ$ and 60° . The final fibre volume content was approximately 52%. The specimens used were DCB type, cut out in a plate thickness equal to 5 mm, containing 16 plies. A Teflon film (30 μm in thickness) was incorporated at the mid-plane of the specimen to initiate the delamination (**Figure 1**).

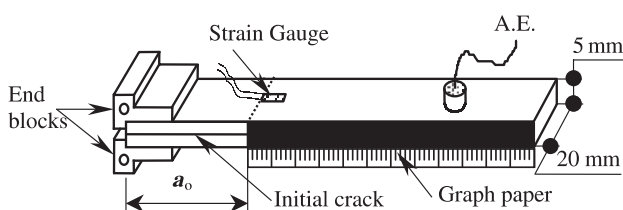


Figure 1: DCB Specimen
Slika 1: DCB-preizkušane

A 5-mm strain gauge and a sensor for acoustic emission were instrumented in each specimen for the detection of the start of delamination. Before loading, the specimens were polished on their two sides, then painted with black ink and a piece of graph paper was stuck on (**Figure 1**). During the loading, an optical fibre was used to light the crack head and binoculars were used to follow the crack development on the two sides of the specimen. The tests were performed in displacement control at a rate of 2 mm/min for the continuous tests and 0.5 mm/min for the loading-unloading tests

3 START OF DELAMINATION

3.1 Mode of starting of the delamination

In this study we chose an experimental methodology that associates microscopic observations to the used instrumentation. The methodology consists of loading a specimen of each type of sequence, and stopping the loading when an acoustic signal appears, then to unload the specimen and observe the edges under a scanning electron microscope (SEM), if there is delamination. However, while unloading, the micro-cracks can be closed again and become difficult to detect if the arms of the specimen are not kept open. We introduced, then, a small plastic hold of small thickness between the arms of the specimen before reducing the load to zero and to prevent the crack from closing again.

We found that for the configurations $\pm 15^\circ, \pm 30^\circ$ and $\pm 45^\circ$, the phenomenon of damage corresponding to the starting of the acoustic signal is an initiation of the delamination occurring in the median plane, **Figure 2**. On the other hand, for the configuration $\pm 60^\circ$, the initial damage is a transverse cracking of one of the two median plies, **Figure 3**. Thus for this last configuration ($\pm 60^\circ$), the initiation of delamination is already preceded by transverse cracking. So, it is necessary to avoid the appearance of transverse cracking before the start of delamination by decreasing the deformation by bending through the increase of the bending rigidity, i.e., the increase of the specimen thickness.

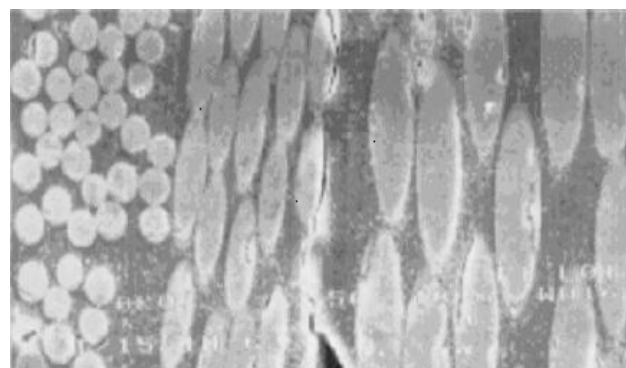


Figure 2: Start of damage by delamination in $\pm 15^\circ$ sequence
Slika 2: Začetek delaminacije v sekvenci $\pm 15^\circ$

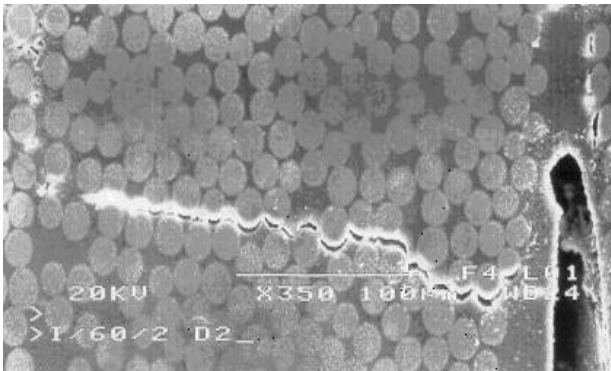


Figure 3: Start of damage by transverse cracking in $\pm 60^\circ$ sequence
Slika 3: Začetek poškodbe s prečnim pokanjem v sekvenci $\pm 60^\circ$

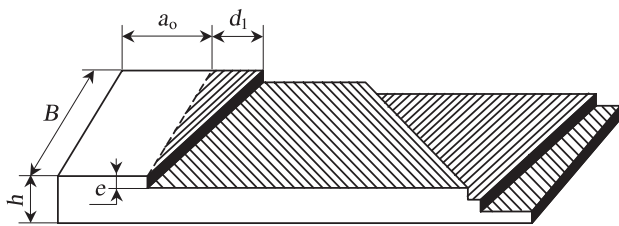


Figure 4: fracture mode of DCB specimen for a $[(\pm\theta)_2]_{2sym}$ sequence ($33,5^\circ < \theta < 67,5^\circ$)

Slika 4: Način preloma DCB-preizkušanca za $[(\pm\theta)_2]_{2sim}$ -sekvenco ($33,5^\circ < \theta < 67,5^\circ$)

3.2 Critical energy release rate

The determination of the critical energy release rate G_{IC} (energy of cracking initiation) was based on the compliance method of Irwin-Kies¹⁴ and the approach of Berry¹⁵. The G_{IC} values obtained are identical for all the used stratification sequences ($\approx 185 \text{ J/m}^2$), therefore G_{IC} is independent of the stratification sequence.

4 PROPAGATION

The experimental tests carried out highlighted two modes of fracture: a delamination in the median plane for the angles $\pm 15^\circ$ and $\pm 30^\circ$; and a fracture illustrated by **Figure 4** for the angles $\pm 45^\circ$ and $\pm 60^\circ$ (delamination in staircases).

Thus, the mode of fracture of the multi-directional laminates subjected to an opening mode is not a pure delamination mode I, as in the case of the unidirectional laminates, but a mixed mode (I+II+III), which depends on the angle θ , and whose modal separation is extremely complex to carry out.

4.1 Propagation energy

During the propagation, the fracture is made almost at the interfaces. Consequently, the energy release rate in propagation G_{IP} depends on the stratification sequence. Three calculation methods were used for the determination of the energy release rate of propagation: i) the technique of the *R*-curve, ii) the compliance method by loading/unloading, and iii) the area method. We present here, for illustration, the results of the *R*-curve method applied for the various sequences of stratification, see **Figure 5**.

The G_{IP} curves obtained by the various methods show that they evolve in the same way according to the crack propagation, i.e., they expressed exactly the same phenomenon. However, only the $\pm 15^\circ$ sequence gives practically identical values for the three methods. For the other sequences, especially $\pm 45^\circ$ and $\pm 60^\circ$, although the three methods give curves with the same trend, the values of G_{IP} change from one method to another.

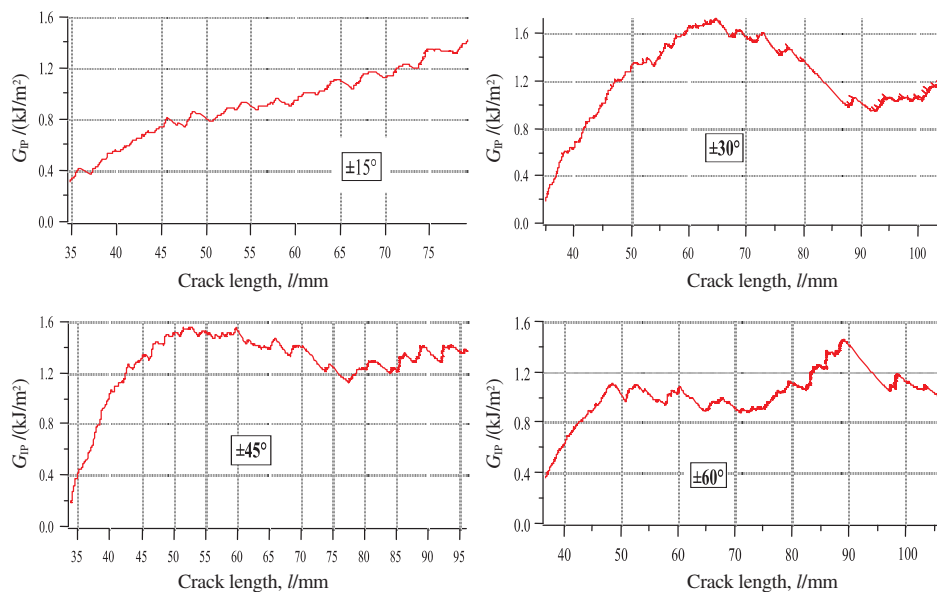


Figure 5: *R*-curves for the various sequences
Slika 5: *R*-krivulje za različne sekvence

4.2 Analysis of the fracture surface

The fracture surface under mode I delamination, in the $\pm 15^\circ$ and $\pm 30^\circ$ sequences, is characterized by two distinct zones. The first zone consists of cohesive fracture zones located mainly at the centre of the specimen and fracture interfaces zones located near the free edges. The cohesive fracture is materialized by a very smooth fracture surface associated with cleavage markings. However, these cleavage markings are not oriented towards the global direction of the propagation, see **Figure 6**. They start perpendicularly to the crack front. The zone of interfaces fracture is materialized by the fibres' imprint near one specimen edge and by the exposed fibre near the other edge. The second zone is made up by a majority of zones of exposed fibres and fibre imprints. The remainder of the zone is made up of small zones of cohesive fracture located in the resin-rich zones and some fibre breakage, **Figure 7**. However, it should be noted that the rate of fibre breakage is more significant in the case of the $\pm 30^\circ$ than in the case of the $\pm 15^\circ$.

The same damage mechanisms observed in the case of the $\pm 15^\circ$ and $\pm 30^\circ$ are present in the case of the $\pm 45^\circ$ and $\pm 60^\circ$. However, the fibre breakage rate is more significant in this last case. A new phenomenon consisting of the observation of cusps formed between the fibres is recorded only in the case of the $\pm 45^\circ$, **Figure 8**. These cusps represent a shear fracture. Another phenomenon is observed only in the case of the $\pm 60^\circ$, which is about the disintegration of the resin, **Figure 9**.

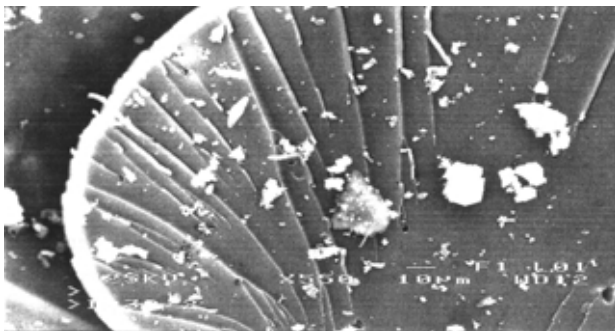


Figure 6: Orientation of cleavage markings
Slika 6: Orientacija znakov cepljenja

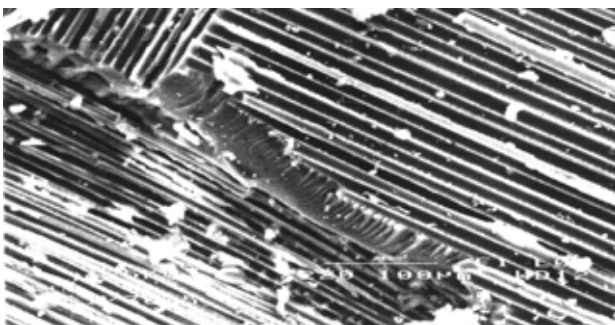


Figure 7: Cohesive fracture zone
Slika 7: Področje kohezivnega preloma

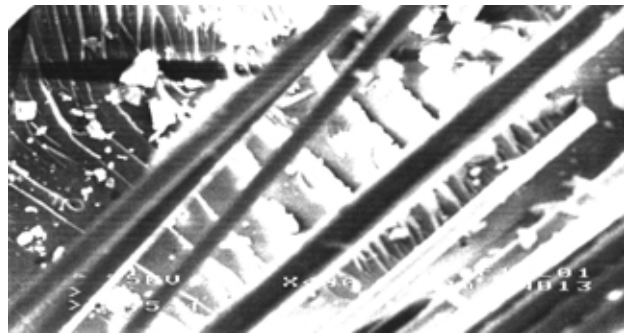


Figure 8: Shearing cusps in the $\pm 45^\circ$ sequence
Slika 8: Strižni žlebovi pri sekvenci $\pm 45^\circ$

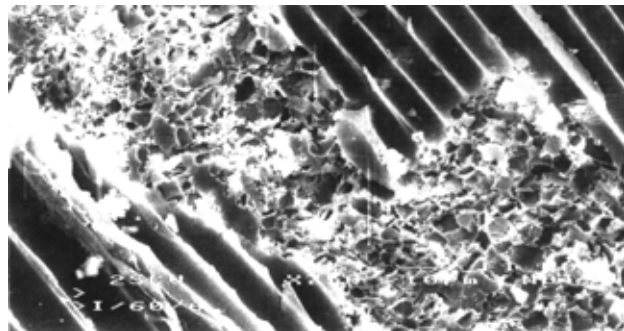


Figure 9: Resin disintegration in the $\pm 60^\circ$ sequence
Slika 9: Prelom smole pri sekvenci $\pm 60^\circ$

5 THICKNESS OPTIMISATION OF THE DCB SPECIMEN

We have experimentally found that for the $\pm 60^\circ$ configuration of 5 mm thickness, the initiation of delamination is already preceded by transverse cracking. So, any calculation of the critical energy release rate will be erroneous because it will contain an amount of energy dissipated by the transverse cracking.

In a previous study³ we used strain gauges, as shown in **Figure 10**. We see that the gauges begin to be loaded as soon as they are at a distance of approximately 10 mm from the crack tip. This distance (10 mm) would correspond to a compression zone located just ahead of the crack tip, and is generally met on the external part of the arms of a specimen loaded in opening mode. It moves, in the form of wave, forwards with a speed equal to that of the projection of the crack tip. The length of

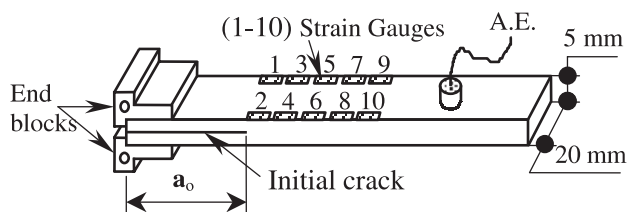


Figure 10: Instrumentation of the DCB specimen by strain gauges and acoustic emission

Slika 10: Inštrumentacija DCB-preizkušanca z merilnimi trakovi za deformacijo in akustično emisijo

this wave depends on the mechanical and geometrical characteristics of the arm. This report enables us to confirm that the arms of the DCB specimen are not embedded perfectly at the crack tip. The calculated energy release rate will be by excess, because it will contain an energy deployed ahead of the crack tip. To cancel these problems, it is necessary to avoid the appearance of transverse cracking before the start of the delamination and to seek the maximum decrease of these strains ahead of the crack tip by increasing the specimen bending rigidity, i.e., its thickness.

5.1 Deformation of the material ahead of the crack tip

Some studies relating to the evaluation of the angle of deflection, at the crack tip, of the arms of the DCB specimen (isotropic material) were undertaken¹⁰⁻¹². They were all based on the Timoshenko beam theory, resting on an elastic foundation. Half of the DCB specimen can be schematised by a semi-infinite beam, of which the part located ahead of the crack tip rests on an elastic foundation (second half of the specimen), and is subjected to a loading concentrated at its free end, **Figure 11**.

A calculation based on the work of Kanninen¹⁶ allowed us to determine the equation of deflexion of half of the DCB specimen, i.e.,

$$y(z) = \frac{Pe^{-\beta z}}{2\beta^3 E_L I_{xx}} (\beta a_0 (\cos \beta z + \sin \beta z) - (\cos \beta z)) \quad (1)$$

With $\beta = \sqrt[4]{\frac{6E_T}{E_L h^4}}$ (2)

The evolution of the deformation d of half of the DCB specimen, the part ahead of the crack tip, of the various configurations is represented by **Figure 12**. The experimental load P taken in the calculation of these deformations corresponds to the initiation of the delamination for each sequence of stratification, for an initial crack length $a_0 = 25$ mm, a width $b = 20$ mm and a thickness $h = 2.5$ mm. **Figure 12** shows that the specimen thickness has a significant effect on both the deformation intensity and the width d of the zone deformed ahead of the crack tip. The existence of a strain field located ahead of the crack tip means that

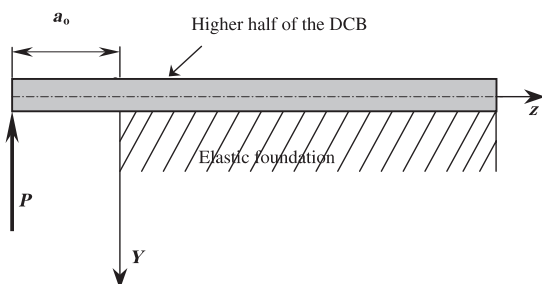


Figure 11: Schematic of a DCB specimen arm
Slika 11: Shema roke DCB-preikušanca

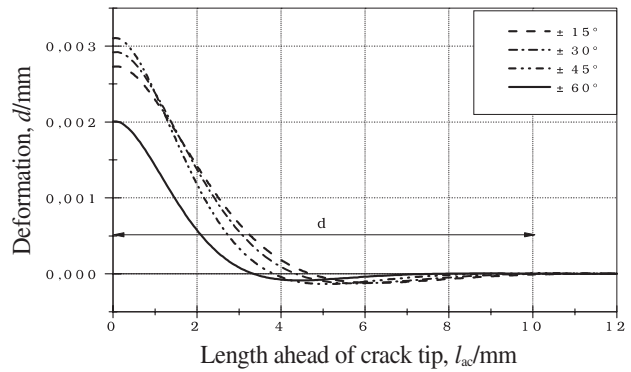


Figure 12: Deformation of the various sequences
Slika 12: Deformacija pri raznih sekvencah

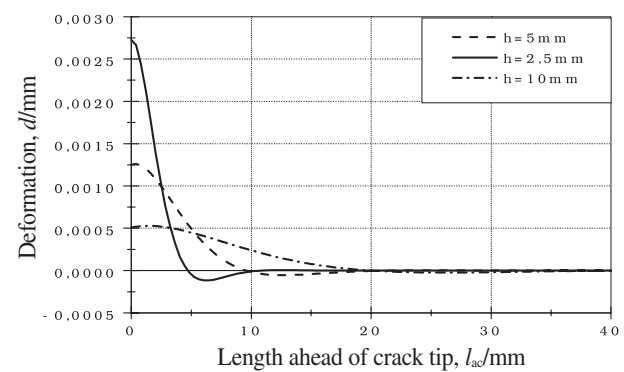


Figure 13: Thickness effect on deformation ahead of the crack tip
Slika 13: Vpliv debeline na deformacijo v konici razpoke

perfect clamping cannot be achieved at the crack tip, but rather at a distance d .

The effect of the arm thickness of the specimen on the deformation field ahead of the crack tip is illustrated by the curves in **Figure 13**, where for the same sequence of stratification, the extent of deformation d goes from 10 mm for $h = 2.5$ mm to 20 mm for $h = 5$ mm and 40 mm for $h = 10$ mm. **Figure 13** shows that the distribution of deformation according to the length ahead of the crack tip changes with the specimen thickness. However, the surface area under the curve remains constant. Thus, by increasing the thickness of the arms, one can reduce the intensity of the deformation until any form of dissipation of energy in this zone is avoided.

5.2 Non linearities

On the basis of Carlson's work¹³, the non-linearities are due primarily to large displacements and cracking by bending. They are expressed by the maximum slope of the deflection y'_m at the point of load application and by the maximum strain ϵ_m corresponding to the fracture by bending. These two parameters will be calculated on the basis of the static diagram of a DCB arm, **Figure 14**. The non-linearities are satisfied for

$$y'_m \leq y'_a \text{ and } \epsilon_m \leq \epsilon_a,$$

where y'_a and ϵ_a are the acceptable values.

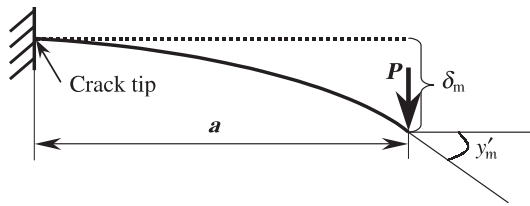


Figure 14: Static diagram of a DCB arm
Slika 14: Statičen diagram DCB-roke

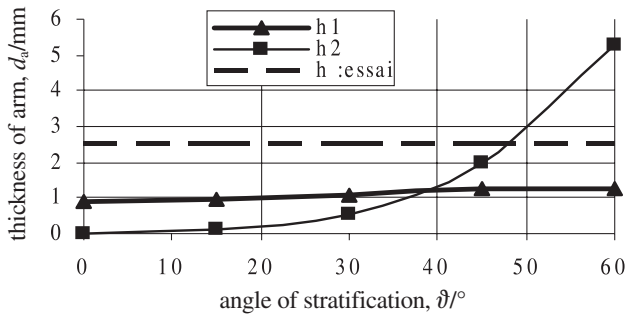


Figure 15: Optimization thickness of the arm of DCB specimen
Slika 15: Optimizacija debeline roke DCB-preizkušanca

These two conditions of non-linearity give the minimum thickness as

$$h \geq \sqrt[3]{\frac{3a^2 G_{IC}}{E y'_a}} \quad (\text{for a large displacement}) \quad (3)$$

and

$$h \geq \frac{3G_{IC}}{E \epsilon_a^2} \quad (\text{for fracture by bending}) \quad (4)$$

5.3 Application to the studied laminates

The optimal values of the thickness h were calculated for an initial crack length equal to 25 mm. The values of G_{IC} and ϵ_a , were given in reference ³. The thickness evolution of the DCB specimen arms necessary for the non-appearance of non-linearities before the start of the delamination is illustrated, in terms of the angle of stratification, in **Figure 15**.

For angles less than approximately 38° , the risk of the appearance of a non-linearity for low thicknesses of the arm (approximately 1 mm) will be due to a large displacement. For the angles larger than 38° , it is the non-linearity by transverse cracking that can affect the behaviour. For the case of the thickness considered in this study (2.5 mm), when the angle of the stratification is larger than 47° , there is an appearance of transverse cracking before the start of the delamination. This is in accordance with the experimental results given previously.

6 CONCLUSION

The behaviour analysis in the delamination of multi-directional laminated composites ($\pm\theta$) loaded in

mode I shows the presence of two distinct phases. First, a phase corresponding to the start of the delamination, whose critical energy release rate G_{IC} is intrinsic to the material and does not depend on the orientation of the stratification plies. Second, a phase corresponding to delamination propagation, whose mode of cracking and energy release rate G_{IP} depend primarily on the angle of orientation of the plies. For $\theta \leq 33.5^\circ$, delamination is propagated in a zigzag mode between the interfaces of the two median plies. The exposed fibres and fibre imprint is the key feature of the fracture surface. There is also some fibre breakage and small zones of cohesive fracture. On the other hand, for $33.5^\circ \leq \theta \leq 67.5^\circ$, the delamination is propagated in a staircase, creating an unsymmetrical specimen, which generates a rotation of the specimen in the vertical plane and a shear loading at the crack tip. Consequently, the stress cannot be considered pure mode I. Rather, it is a mixed mode (I+II) and sometimes a mixed mode (I+II+III) because of the intra-laminar fracture.

The experimental results showed the existence of a strain field ahead of the crack tip, which explains why the clamping is not as perfect as was supposed. The analytical results obtained are in perfect agreement with the experimental results, and allowed us to determine the minimum thickness of the DCB specimen, which satisfies the application of the concept of the linear elastic fracture mechanics (LEFM).

7 REFERENCES

- Ahmed Benyahia A, Laksimi A, Benmedakhene S, Gong X L. Fracture process in $\pm\theta$ laminates subjected to mode II Loading. *Strength of Materials*; 34 (2002) 4, 390–401
- Laksimi A., Ahmed Benyahia A., Benzeggagh M. L., Gong X. L., Initiation and bifurcation mechanisms of cracks in multidirectional laminates, *Composites Science and Technology*, 60 (2000), 597–604
- Ahmed Benyahia A. Etude des mécanismes de délaminage sous l'effet de contraintes complexe générées par des sollicitations simples d'ouverture et de cisaillement dans les stratifiés $\pm\theta$. PhD Thesis, Université de Technologie de Compiègne, 1997
- Russel A. J., K. N. Street, Factors affecting the inter-laminar fracture energy of Graphite/Epoxy laminates, *Progress in Science and Engineering of Composites*, J. Hayashi, K. Kawata & S. Umekawa, Ed., ICCM-IV, Tokyo, 1982, 279–300
- D. J. Wilkins, J. R. Eismann, R.A. Camin, W.S. Margolis & R.A. Benson, Characterization delamination growth in graphite/epoxy, *Damage in composite materials*, ASTM STP 775, Philadelphia, 1982, 168–183
- D. J. Nicholls, J. P. Gallagher, Determination of G_{IC} in angle ply composites using a cantilever beam test method, *J. Reinforced Plastics and Composites*, (1983) 2, 2–17
- H. Chai, The characterization of mode I delamination failure in non-woven multidirectional laminates, *Composites*, 15 (1984) 4, 277–290
- I. Chou, I. Cimpara, K. Kageyama & I. Oshawa, Mode I and Mode II fracture toughness measured between differently oriented plies in Graphite/Epoxy Composites, *Composite Materials : Fatigue and Fracture*, Fifth volume, ASTM STP 1230, R.H. Martin, ED., ASTM, Philadelphia, 1995, 132–151
- Williams J. G. Mode I transverse cracking in an epoxy and graphite fiber reinforced epoxy. M. S. Thesis, Texas A&M University, 1981

- ¹⁰Williams J. G., End corrections for orthotropic DCB specimen. *Composites Science and Technology*; 35 (1989), 367–376
- ¹¹Penado F. E., A closed form solution for the energy release rate of the double cantilever beam specimen with an adhesive layer. *Journal of Composite Materials*; 27 (1993) 4, 383–407
- ¹²Olsson R., A simplified improved beam analysis of the DCB specimen. *Composites Science and Technology*; 43 (1992), 329–338
- ¹³Carlsson LA, Gillespie JW, Pipes JR, Pipes RB. On the analysis and design of End Notched Flexure (ENF) specimen for mode II testing. *Journal of Composite Materials*; 20 (1986), 594–604
- ¹⁴G. R. Irwin, J. A. Kies, Critical energy rate analysis of fracture strength, *Welding Research supplement*, 19 (1954), 193–198
- ¹⁵J. P. Berry, Determination of fracture surface energies by the cleavage technique, *J. of App. Phys.*, 34, 62–68
- ¹⁶Kanninen MF., An augmented double cantilever beam model for studying crack propagation and arrest, *International Journal of Fracture*; 9 (1973), 83–92